

LARGE ZENITH ANGLE OBSERVATION OF THE HADRONIC PEVATRON CANDIDATE SNR G106.3+2.7 WITH LST-1 AND MAGIC

M.-S. Carrasco¹, F. Cassol¹, H. Costantini¹, G. Emery¹, T. Saito², C. Arcaro³ and M. Pihet⁶

Abstract. The quest for PeVatrons, sources of Galactic cosmic rays accelerated up to PeV energies, lived an exciting development with the recent discoveries from the LHAASO Collaboration. Published in 2023, the first LHAASO catalog of Gamma-Ray sources presents 43 sources of ultra-high energy emissions (UHE, $E > 100$ TeV). Among them, a promising hadronic PeVatron candidate is the supernova remnant SNR G106.3+2.7, for which the ultra-high energy emission has been interpreted using both hadronic and leptonic scenarios.

Imaging Atmospheric Cherenkov Telescopes (IACTs) are ideal instruments to investigate the nature of extended sources in the gamma-ray domain thanks to their better angular and energy resolution compared to UHE detectors. Using the LST-1, the first Large-Sized Telescope of the Cherenkov Telescope Array Observatory, together with the two neighboring MAGIC IACTs, we are currently observing the SNR G106.3+2.7 at Large Zenith Angle (LZA, zenith = 55°-75°), which allows us to explore the 1-50 TeV energy range.

Such observations raise challenges regarding the data reconstruction and analysis, due to the zenith angle dependency of the Random Forest-based reconstruction and of the telescope acceptance. In this contribution, we will present preliminary results, including a first morphological and spectral analysis of the source.

Keywords: CTA, LST-1, MAGIC, Cherenkov telescope, PeVatron, supernova remnant, large zenith angle

1 Introduction

SNR G106.3+2.7 is a supernova remnant (SNR) recently confirmed to be a PeVatron by LHAASO, which measured emissions up to ~ 600 TeV (cf. Fig. 1 Left) (Cao et al. 2024, 2021). In radio it has the shape of a comet, characterized by a head with higher brightness and a fainter elongated tail (cf. Fig. 1 Right) (Kothes et al. 2001). The head region is colliding with a dense HI cloud and appears to contain the energetic pulsar (PSR) PSR J2229+6114 and its associated pulsar wind nebula (PWN), also known as the Boomerang Nebula. The tail region is expanding in a low density HI cavity, located in the vicinity of a dense molecular cloud.

Due to LHAASO's low angular resolution and the complex nature of the SNR, the origin of the UHE emission is still unknown. Signal from the head region could be associated to the PSR and PWN and make the SNR a leptonic PeVatron, whereas signal from the tail region could be correlated with the molecular cloud and make it a hadronic PeVatron. The source, discovered in the early 90's (Joncas & Higgs 1990), has been subject to extensive multi-wavelength (MWL) campaigns since (Albert et al. 2020; Amenomori et al. 2021; De Sarkar et al. 2022; Fang et al. 2022; Liu et al. 2022; Pope et al. 2023). So far, no MWL spectral analysis was able to determine the leptonic or hadronic nature of SNR G106.3+2.7. Hadronic emission models tends to be favored, but the leptonic scenario has not been ruled out. Recently, MAGIC presented results which indicate energy dependent emission morphology at Very High Energy (VHE, $E > 100$ TeV) (cf. Fig. 2 Left). We aim to investigate these results with increased detection efficiency at high energies (> 10 TeV), which is achieved with Large Zenith Angle (LZA, zenith = 55°-75°) pointing and with joint LST-1 and MAGIC observations (cf. Fig. 2 Right).

¹ Aix Marseille Univ, CNRS/IN2P3, CPPM, Marseille, France

² ICRR, Tokyo, Japan

³ INFN, Padova, Italy

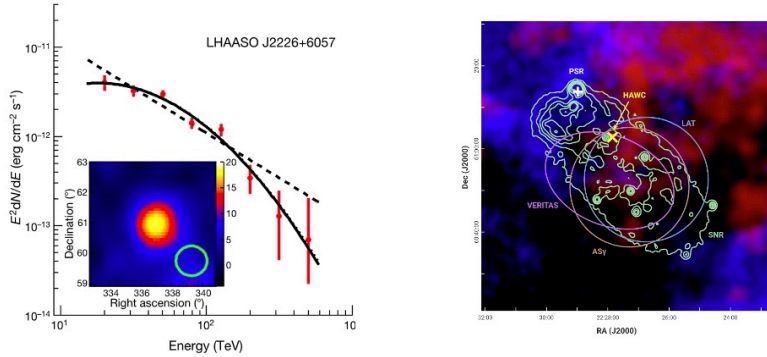


Fig. 1. **Left:** LHAASO J2226+6057 spectrum and significance map. The source was associated to SNR G106.3+2.7, making it a confirmed PeVatron (Cao et al. 2021). **Right:** SNR G106.3+2.7 1.4 GHz radio contours with its surrounding gas environment. The comet shaped SNR is described as having its head region in collision with a dense HI cloud (blue) and its tail region in expansion within a low density HI cavity (black), in the vicinity of a dense molecular cloud (red, CO emissions) (Ge et al. 2021).

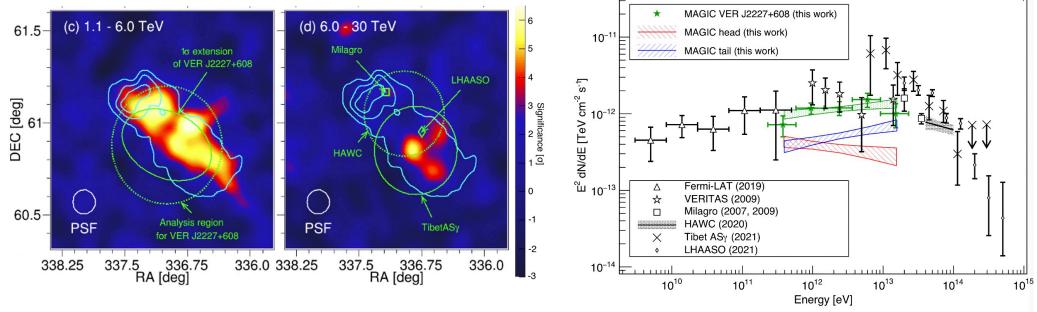


Fig. 2. **Left:** Significance maps of SNR G106.3+2.7 observed by MAGIC for the 1.1-6 TeV and 6-30 TeV energy bins, showing the energy-dependent morphology of the source (MAGIC Collaboration et al. 2022). **Right:** Spectral energy distribution of SNR G106.3+2.7 gamma emissions detected by MAGIC, *Fermi*-LAT, VERITAS, Milagro, HAWC, Tibet AS γ and LHAASO (MAGIC Collaboration et al. 2022).

2 LZA observation with LST-1 and MAGIC

SNR G106.3+2.7 is currently undergoing a multi-year observation campaign with LST-1 and the two MAGIC telescopes, with a final target time of 120 hours. Imaging Atmospheric Cherenkov Telescopes (IACTs) are known for their optimal angular and energy resolution when compared to UHE detectors.

Joint LST-1-MAGIC observations are obtained with a simultaneous pointing to the source and a joint data reconstruction. Images are connected by a software trigger, which requires at least two telescope images per event. The improvement of the flux sensitivity is around 30% with respect to MAGIC only observations (Abe et al. 2023). We perform our observation at LZA in order to increase the effective area at higher energies (Acciari et al. 2020).

Fig. 3 shows the performance of LST-1-MAGIC for zenith angles ranging from 61° to 74°. The effective area at the highest zenith angle is increased by a factor ~ 3 at 10 TeV and up to ~ 7 at 50 TeV. The angular resolution is below 0.1° and the energy resolution $\sim 15\%$ for energies above 10 TeV for all zeniths.

3 Data analysis

The source has been observed in wobble mode, with two pointings positioned in a way to study both the head and the tail regions. The final dataset will be a combination of mono LST-1, stereo MAGIC and joint stereo LST-1+MAGIC datasets, which are reconstructed with their respective pipelines: *lstchain*, *MARS* and *magic-cta-pipe* (Abe et al. 2023; López-Coto et al. 2020; Zanin et al. 2013). The Random Forests used for reconstruction were trained on Monte-Carlo data simulated along the declination line with a dense grid of

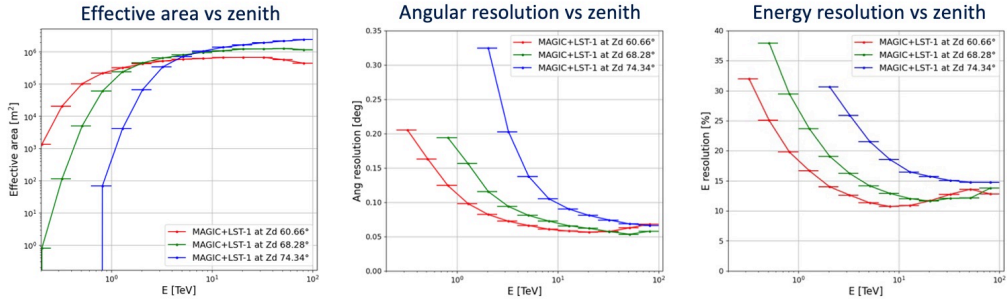


Fig. 3. Expected performances for LST-1+MAGIC joint observation at large zenith angle (LZA) of SNR G106.3+2.7 for three zeniths: 60.66°(red), 68.28°(green) and 74.34°(blue). The effective area is increased at the highest energies, at the expense of a heightened energy threshold and resolution degradation at the lower energies. The computation was obtained with Monte-Carlo simulation of stereo data reconstructed with `magic-cta-pipe`.

pointings in order to reduce the bias induced by the fast-varying shower parameters at LZA. The high level analysis was performed with `gammam` (Deil et al. 2017).

In this contribution, we present very preliminary results obtained with 38 hours of LST-1 data only, with sky-maps and energy-spectrum obtained through a point-like source analysis. The 1D spectral analysis was performed in a ON region (0.2°radius) centered on the source tail position estimated by MAGIC (RA= 336.72°, DEC=60.84°). The emission spectrum was modelled with a power law function given by $\frac{dN}{dE} = N_0(\frac{E}{3\text{TeV}})^{-\Gamma}$. The spectral points were computed requiring a minimum of 2σ significance.

At LZA the rapidly changing atmosphere depth implies an inhomogeneous acceptance in the telescope field of view (FoV), which is 4.5°for LST-1 and 3.5°for MAGIC. Its modelling was performed with the `acceptance_modelisation` package*. The acceptance model was then used in the ring background method (Abdalla et al. 2018) which was employed to produce the skymaps. The spectral analysis was performed with the reflected background method (Berge et al. 2007). This method doesn't take into account the acceptance differences between the ON and the OFF regions, which will be improved in future studies by using the acceptance corrected background estimation.

4 Results

4.1 Energy-dependent morphology

Fig. 4 Left and Fig. 5 show the skymaps obtained for the 1-70 TeV, 1-10 TeV, and 10-70 TeV energy ranges. Looking at all events ($E > 1$ TeV), we see emissions from the center region of the SNR and from the tail region. We begin to see a shift towards the tail for higher energies. We detect the source up to 5σ for $E < 10$ TeV and above 4σ for $E \geq 10$ TeV. These results are consistent with those published by MAGIC (cf. Fig. 2 Left; from (MAGIC Collaboration et al. 2022)).

4.2 Spectral analysis

Fig. 4 Right shows the spectral energy distribution obtained from the tail region fitted with a power law. The best-fit parameters are shown in Tab. 1. The spectral index is consistent with LHAASO's WCDA results, while the flux normalization at 3 TeV is consistent with MAGIC's result, although the ON region radius is slightly different. With 38 hours we were able to obtain 4 spectral flux points in the 1.1 - 70 TeV energy range.

5 Conclusions

SNR G106.3+2.7 is undergoing a multi-year observation campaign at LZA with LST-1 and MAGIC telescopes. We performed a preliminary analysis on a total of 38 hours of LST-1 data taken with a zenith angle between 55°and 75°. We detected the source at 5σ up to 10 TeV with two emission regions, one in the tail and one closer

*https://github.com/mdebony/acceptance_modelisation

to the head. The source was detected at more than 4σ at $E > 10$ TeV, with an apparent shift of the emission site towards the tail. Both energy-dependent morphology and spectral analysis preliminary results were consistent with MAGIC and LHAASO's results. The joint observation campaign is ongoing and joint LST-1 and MAGIC results will be available soon.

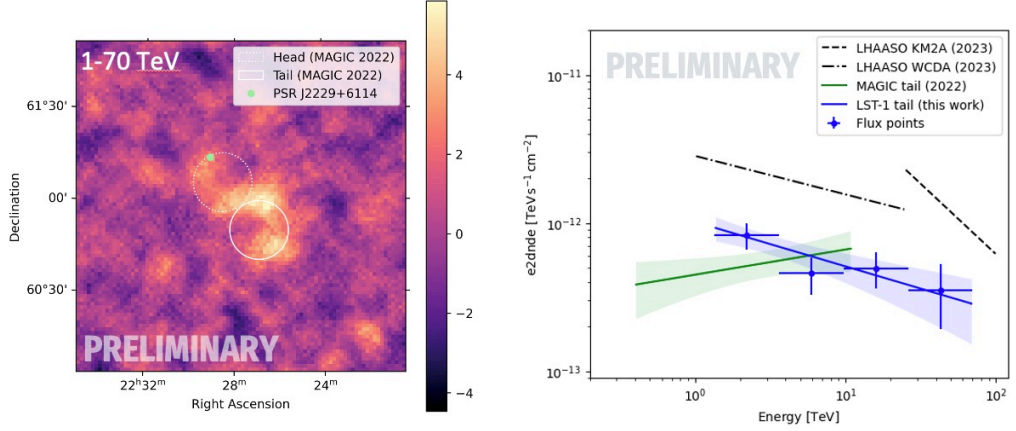


Fig. 4. Left: Significance map of the SNR G106.3+2.7 region observed by LST-1 at LZA between 1 and 70 TeV. Right: Differential energy spectrum of the source fitted with a power law over a 0.2° radius ON region centered on MAGIC's tail position. The shaded band corresponds to the range of the power-law fit (68% confidence level), taking into account statistical errors. LHAASO and MAGIC results are shown for reference (cf. Tab. 1) (Cao et al. 2024; MAGIC Collaboration et al. 2022).

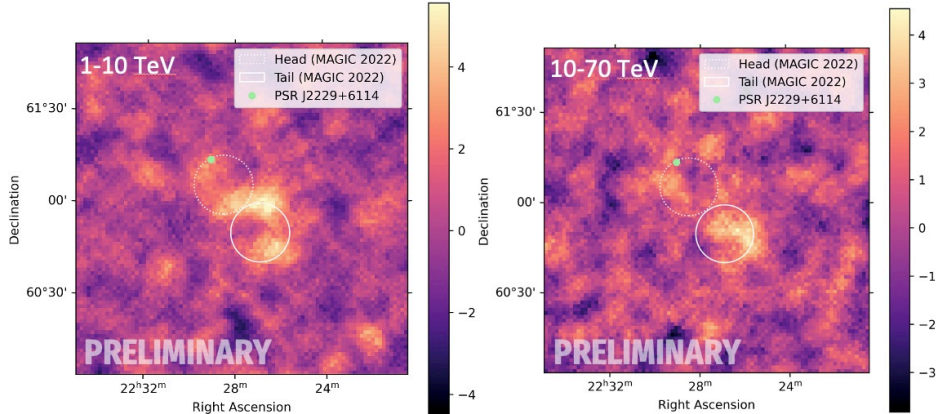


Fig. 5. Significance maps of the SNR G106.3+2.7 region observed by LST-1 at LZA in the 1-10 TeV and 10-70 TeV energy bins.

Source	ON region radius (°)	$N_0 (10^{-14} \text{ cm}^{-2} \text{ s}^{-1} \text{ TeV}^{-1})$ at 3 TeV	Γ
LST-1 tail	0.2	8.13 ± 1.20	2.30 ± 0.14
MAGIC tail	0.16	$6.0 \pm 0.7_{\text{stat}} \pm 1.0_{\text{sys}}$	$1.83 \pm 0.10_{\text{stat}} \pm 0.15_{\text{sys}}$
1LHAASO J2228+6100u (KM2A)	3	4.76 ± 0.14	2.95 ± 0.04
1LHAASO J2228+6100u (WCDA)	3	2.37 ± 0.16	2.26 ± 0.04

Table 1. Best fit parameters obtained for the spectral analysis of SNR G106.3+2.7 tail region as described in Sec. 3 and shown in Fig. 4 Right, with MAGIC and LHAASO results for reference (Cao et al. 2024; MAGIC Collaboration et al. 2022).

References

Abdalla, H., Abramowski, A., Aharonian, F., et al. 2018, *Astronomy & Astrophysics*, 612, A1

Abe, H., Abe, K., Abe, S., et al. 2023, *Astronomy & astrophysics*, 680, A66

Acciari, V. A., Ansoldi, S., Antonelli, L., et al. 2020, *Astronomy & Astrophysics*, 635, A158

Albert, A., Alfaro, R., Alvarez, C., et al. 2020, *The Astrophysical Journal Letters*, 896, L29, publisher: The American Astronomical Society

Amenomori, M., Bao, Y. W., Bi, X. J., et al. 2021, *Nature Astronomy*, 5, 460, number: 5 Publisher: Nature Publishing Group

Berge, D., Funk, S., & Hinton, J. 2007, *A&A*, 466, 1219

Cao, Z., Aharonian, F., An, Q., et al. 2024, *The Astrophysical Journal Supplement Series*, 271, 25

Cao, Z., Aharonian, F. A., An, Q., et al. 2021, *Nature*, 594, 33, number: 7861 Publisher: Nature Publishing Group

De Sarkar, A., Zhang, W., Martín, J., et al. 2022, LHAASO J2226+6057 as a pulsar wind nebula, arXiv:2209.13285 [astro-ph]

Deil, C., Zanin, R., Lefaucheur, J., et al. 2017, arXiv preprint arXiv:1709.01751

Fang, K., Kerr, M., Blandford, R., Fleischhack, H., & Charles, E. 2022, *Physical Review Letters*, 129, 071101, arXiv:2208.05457 [astro-ph]

Ge, C., Liu, R.-Y., Niu, S., Chen, Y., & Wang, X.-Y. 2021, *The Innovation*, 2, publisher: Elsevier

Joncas, G. & Higgs, L. A. 1990, *Astronomy and Astrophysics Supplement Series*, 82, 113

Kothes, R., Uyaniker, B., & Pineault, S. 2001, *The Astrophysical Journal*, 560, 236

Liu, Q.-C., Zhou, P., & Chen, Y. 2022, *The Astrophysical Journal*, 926, 124, publisher: The American Astronomical Society

López-Coto, R., Baquero, A., Bernardos, M. I., et al. 2020, in 30th Astronomical Data Analysis Software and Systems, Vol. 532, Astronomical Society of the Pacific, 357

MAGIC Collaboration, Abe, H., Abe, S., et al. 2022, MAGIC observations provide compelling evidence of the hadronic multi-TeV emission from the putative PeVatron SNR G106.3+2.7, arXiv:2211.15321 [astro-ph]

Pope, I., Mori, K., Abdelmaguid, M., et al. 2023, A multi-wavelength investigation of PSR J2229+6114 and its pulsar wind nebula in the radio, X-ray, and gamma-ray bands, arXiv:2310.04512 [astro-ph]

Zanin, R., Carmona, E., Sitarek, J., et al. 2013, in Proc. of the 33st International Cosmic Ray Conference, Rio de Janeiro, Brasil